



The ubiquitin ligase COP1 regulates cell cycle and apoptosis by affecting p53 function in human breast cancer cell lines

Won Hye Ka^{1,2} · Seok Keun Cho³ · Byung Nyun Chun¹ · Sang Yo Byun² · Jong Cheol Ahn¹

Received: 17 October 2017 / Accepted: 23 February 2018
© The Japanese Breast Cancer Society 2018

Abstract

Background The E3 ubiquitin ligase constitutive photomorphogenic 1 (COP1) mediates cell survival, growth, and development, and interacts with the tumor suppressor protein p53 to induce its ubiquitination and degradation. Recent studies reported that COP1 overexpression is associated with increased cell proliferation, transformation, and disease progression in a variety of cancer types. In this study, we investigated whether COP1 regulates p53-mediated cell cycle arrest and apoptosis in human breast cancer cell lines.

Methods We downregulated *COP1* expression using lentiviral particles expressing short hairpin RNA (shRNA) targeting *COP1* and measured the effects of the knockdown in three different breast cancer cell lines.

Results *COP1* silencing resulted in p53 activation, which induced the expression of *p21* and p53-upregulated modulator of apoptosis (PUMA) expression, and reduced the levels of cyclin-dependent kinase 2 (CDK2). Notably, knockdown of *COP1* was associated with cell cycle arrest during the G₀/G₁ phase.

Conclusions The COP1-mediated degradation of p53 regulates cancer cell growth and apoptosis. Our results indicate that COP1 regulates human breast cancer cell proliferation and apoptosis in a p53-dependent manner. These findings suggest that COP1 might be a promising potential target for breast cancer-related gene therapy.

Keywords COP1 · p53 · RNA silencing · Gene therapy

Introduction

Breast cancer (BC) is the second leading cause of cancer-related death in women worldwide. Conventional chemotherapy induces significant side effects, because it targets all proliferating cells. To identify new and effective therapeutic

strategies, it is necessary to fully elucidate the cancer-specific signaling mechanisms. Inactivation of the tumor suppressor p53 is a major factor that contributes to BC development [1–5].

p53 mutation, which is mutated/lost in many human cancers [6], promotes both growth arrest and apoptosis-related gene expression in response to various signals, thereby mediating the downstream pathways that regulate these processes [7–9]. Specifically, p53 mediates a variety of stress signals by activating the transcription of genes involved in angiogenesis, cell cycle arrest, apoptosis, and DNA repair. The physiological consequences of p53 activation include growth arrest and apoptosis, which prevent cells from replicating genetically damaged genomes [8]. The cyclin-dependent kinase (CDK) inhibitor p21 is the primary mediator of p53 function; studies have demonstrated that p21 blocks cell cycle progression at the G₁/S stage [9] and plays a critical role in modulating CDK2 activity [10, 11]. The proliferation of mammalian cells is controlled by the combined action of CDK4 and CDK2 during the G₁ phase of the cell cycle. Additionally, in case of severe DNA damage,

✉ Sang Yo Byun
sybyun@ajou.ac.kr

✉ Jong Cheol Ahn
jcahn@woojungbsc.co.kr

¹ WJ R&D Center, WOJUNG BSC, Advanced Institutes of Convergence Technology, 145 Gwanggyo-ro, Yeongtong-gu, Suwon-si, Gyeonggi-do 443-270, Republic of Korea

² Applied Biotechnology Department, Ajou University, 206 Worldcup-ro, Yeongtong-gu, Suwon 16499, Republic of Korea

³ Department of Systems Biology, College of Life Science and Biotechnology, Yonsei University, 50 Yonsei-ro Seodaemun-gu, Seoul 03722, Republic of Korea

p53 induces the expression of several apoptotic regulators, including p53-upregulated modulator of apoptosis (PUMA), Bcl-2-associated X protein, and phorbol-12-myristate-13-acetate-induced protein 1, and causes programmed cell death [8]. The p53 pathway is inactivated by somatic mutations in ~50% of human cancers, indicating its importance in maintaining genomic stability [3]. The overall frequency of p53 mutations in BC is ~20%, suggesting that various other mechanisms are involved in inactivating p53-related functions [4, 5].

In non-cancerous cells, the activity of p53 is modulated by constitutive photomorphogenic 1 (COP1), an E3 ubiquitin ligase that contains RING-finger, coiled-coil, and WD40-repeat domains [12, 13]. COP1 was first identified in *Arabidopsis thaliana*, where it mediates light-response functions that are essential for photomorphogenesis in plants [14]; however, its role in mammalian cells is less established. Previous studies have characterized COP1 as both a tumor suppressor and an oncogene [15, 16], and revealed it is involved in important processes related to cancer cell survival, development, and growth. COP1 is also frequently overexpressed in several human cancers [13, 17, 18], including 44% of ovarian adenocarcinomas, 70% of pancreatic cancers, and ~81% of breast adenocarcinomas, as well as hepatocellular carcinomas. Previous immunohistochemical staining of gastric cancer tissues have shown elevated COP1 expression and low p53 expression in the same patients [15, 17, 18]. Due to its ubiquitous expression and correlation with reduced levels of p53 and p21, COP1 is a promising potential diagnostic marker for a variety of BCs.

COP1 interacts with several cancer-related proteins, including E26 transformation-specific (ETS) family [16, 19, 20], c-JUN [21, 22], metastasis-associated protein 1 [21], and forkhead box O1 [22]. Additionally, COP1 and other E3 ubiquitin ligases, including the E3 ubiquitin protein ligase murine double minute 2 (MDM2) and p53-induced RING-h2 protein, mediate the proteasomal degradation of p53 [23, 24]. Although COP1 has been associated with p53 modulation [19, 25], the mechanisms underlying this function in human BC are unclear.

In this study, we investigated the COP1-mediated p53 stabilization and activation in three BC cell lines upon *COP1* knockdown. Our results indicated that *COP1* silencing in p53-wild-type (WT) cell lines stimulated p53 activation, resulting in p53-induced G₀/G₁ cell cycle arrest, increased expression of pro-apoptotic genes such as *p21* and *PUMA*, lowered cycle arrest or apoptosis in p53-null cell lines. These results reveal a novel COP1-mediated p53-dependent pathway associated with the regulation of BC cell proliferation.

Materials and methods

Cell lines and reagents

We used three BC cell lines, including MCF7 (p53-WT and MDM2-overexpressing), ZR-75-1 (p53-WT), and MDA-MB-157 (p53-null), and the non-cancerous human mammary epithelial cells (HMEC; product number PCS-600-010). All cell lines were obtained from the American Type Culture Collection (ATCC, Rockville, MD, USA). MCF7, ZR-75-1, and MDA-MB-157 cells were cultured at 37 °C in a 5% CO₂ incubator in Dulbecco's modified Eagle medium (DMEM), Roswell Park Memorial Institute medium, and Leibovitz's L-15 medium (Thermo Fisher Scientific, Waltham, MA, USA), respectively, supplemented with 10% fetal bovine serum (FBS) (Thermo Fisher Scientific, Waltham, MA, USA) and 1% penicillin/streptomycin (Thermo Fisher Scientific, Waltham, MA, USA). HMEC cells were maintained in mammary epithelial cell basal medium (PCS-600-030; American Type Culture Collection) containing rH-insulin, L-glutamine, epinephrine, apo-transferrin, rH-TGF- α , extractP, and hydrocortisone hemisuccinate (PCS-600-030; American Type Culture Collection). HEK293T cells (Thermo Fisher Scientific, Waltham, MA, USA), used for the production of viral particles, were maintained at 37 °C and 5% CO₂ in DMEM supplemented with 10% FBS and 1% penicillin/streptomycin (Thermo Fisher Scientific, Waltham, MA, USA).

Lentiviral packaging and transduction

Lentiviral vectors expressing non-silencing short hairpin RNA (shRNA)-control sequences (RHS4743; Open Biosystems, Huntsville, AL, USA) were used to generate control lentiviral particles. Lentiviral vectors expressing shRNAs targeting *COP1* (*shCOP1*, TRIPZ RWD2 shRNA; Open Biosystems) were as follows: *shCOP1* #1 (V3THS_354972; mature antisense: TCATTGTATCATCTTCTT); *shCOP1* #2 (V3THS_354971; mature antisense: AGATTGGTA GACCACAGCT); *shCOP1* #3 (V3THS_354970; mature antisense: AGACTTTAATCTTCTTTGT); *shCOP1* #4 (V3THS_354968; mature antisense: TCTTTTCGGTCT TTGTCGA); and *shCOP1* #5 (V2THS_260407; mature antisense: TATAATCTCCATTGGAAGC). Only one of the lentiviral shRNA (*shCOP1* #3) was used in this study, based on the efficiency and specificity of the knockdown. We transfected 5 shRNAs into cells at the same concentration and analyzed expression by RT-qPCR (data not shown).

HEK293T cells (6×10^6) were seeded into 100-mm dishes (Corning, Corning, NY, USA), and after 24 h, were

transfected using Trans-Lentiviral ORF packaging kit with calcium phosphate transfection reagent (#TLP5916; GE Dharmacon™, Lafayette, CO, USA) and 42 µg of the lentiviral vector expressing shCOP1 #3, according to the manufacturers protocol. After 14 h, the transfection mixture was replaced with DMEM supplemented with 5% FBS and, after additional 48 h, the supernatants were harvested and filtered using a 0.45-µm filter (Millipore, Billerica, MA, USA). One volume of cold (4 °C) PEG-it virus-precipitation solution (System Biosciences, Palo Alto, CA, USA) was added to four volumes of lentiviral particle-containing supernatant, and the mixture was centrifuged at 1500g for 30 min at 4 °C. The resulting viral pellet was resuspended in 10 mL DMEM, and the suspension was divided into 10 µL aliquots. Transduction efficiency was determined by seeding HEK293 cells into 96-well plates at a density of 3×10^3 cells/well before addition of 10 µL of lentiviral particles suspension. After 72 h, green-fluorescent protein-positive cells, indicating infected cells, were observed under a fluorescence microscope (Leica, Wetzlar, Germany).

Western blot analysis

Cells were lysed using radioimmunoprecipitation assay buffer (Bio-Rad, Hercules, CA, USA), and the protein content of the cell lysates was measured via a Bradford protein assay. Samples were boiled for 5 min, and 20 µg of proteins were separated by sodium dodecyl sulfate polyacrylamide-gel electrophoresis. The proteins were then transferred to a nitrocellulose membrane and immunoblotted using either an anti-COP1 (1:1000; Abcam, Cambridge, UK), anti-p53 (1:1000; Santa Cruz Biotechnology, Dallas, TX, USA), anti-p21WAF1/CIP1 (1:1000; Cell Signaling Technology, Danvers, MA, USA), anti-PUMA (1:1000; Cell Signaling Technology), or anti-CDK2 (1:1000; R&D Systems, Minneapolis, MN, USA) antibody. An anti-glyceraldehyde 3-phosphate dehydrogenase (GAPDH) antibody (1:2000; Santa Cruz Biotechnology) was used as loading control. The membranes were then incubated with an appropriate horseradish peroxidase-conjugated anti-mouse (1:5000; Santa Cruz Biotechnology), anti-goat (1:5000; Santa Cruz Biotechnology), and/or anti-rabbit (1:6000; Santa Cruz Biotechnology) secondary antibody, and detected using an enhanced chemiluminescence-detection system (Pierce; Thermo Fisher Scientific). Images were obtained using an Image Quant LAS 4000 system (GE Healthcare Life Sciences, Pittsburgh, PA, USA).

Quantitative polymerase chain reaction (qPCR)

BC cells were seeded at a density of 1×10^6 cells/well in 6-well plates and infected (for 72 h at 37 °C) with

lentiviral particles expressing either *shCOP1* or non-silencing shRNA at a multiplicity of infection (MOI) of 10. RNA samples were prepared using an RNeasy mini kit (Qiagen, Valencia, CA, USA), and 100 ng of total RNA was used to measure relative transcript levels via qPCR with the PikoReal real-time PCR system, a Verso 1-step RT-qPCR kit, and SYBR Green (Thermo Fisher Scientific, Waltham, MA, USA). It is a system that synthesizes cDNA directly from RNA using a 1-step kit. qPCR cycling conditions were as follows: 15 min at 50 °C and 40 cycles of denaturation (15 s at 95 °C), annealing (30 s at 58 °C), and extension (30 s at 72 °C). Primer sequences were as follows: *p53* forward, 5'-TAACAGTTCCTGCATGGG CGGC-3', and reverse, 5'-AGGACAGGCACAAACACC CACC-3'; *p21* forward, 5'-CTGGAGACTCTCAGGGTC GAAA-3', and reverse, 5'-GATTAGGGCTTCCTCTTG GAGAA-3'; *GAPDH* forward, 5'-GTCAACGGATTGGT CGTATT-3', and reverse, 5'-GATCTCGCTCCTGGAAGA TGG-3'. Assays were performed in triplicate.

Cell viability and cytotoxicity assays

BC cells (100 µL) were seeded at a density of 1×10^4 cells/well in 96-well plates and infected with either 1, 2.5, 5, or 10 MOI *shCOP1* (or control shRNA) lentiviral particles. After 72 h, the cells were centrifuged, and the supernatants were collected. To measure cell viability, cells were incubated for 4 h at 37 °C and 5% CO₂ in 3-(4,5-dimethylthiazol-2-yl)-2,5-diphenyltetrazolium bromide (MTT) solution (final concentration, 1 mg/mL). Cell toxicity was evaluated using the CytoTox 96 non-radioactive cytotoxicity assay (Promega, Madison, WI, USA) to measure lactate dehydrogenase (LDH) release according to manufacturer instructions.

Flow cytometric analysis of apoptosis

Apoptosis was determined by Annexin V-fluorescein isothiocyanate (FITC)/propidium iodide (PI) staining and visualized using the TACS Annexin V-FITC apoptosis-detection kit (R&D Systems). Briefly, cells were seeded into 6-well plates and treated with *shCOP1* (or control shRNA) lentiviral particles (10 MOI) for 48 h prior to analysis. All cells were collected and prepared for detection according to manufacturer instructions. A total of 1×10^5 events per assay were analyzed using a FACSCalibur flow cytometer (Becton–Dickinson [BD], Franklin Lakes, NJ, USA) and the CellQuest software (BD Biosciences, San Jose, CA, USA). Data were obtained from experiments performed in triplicate.

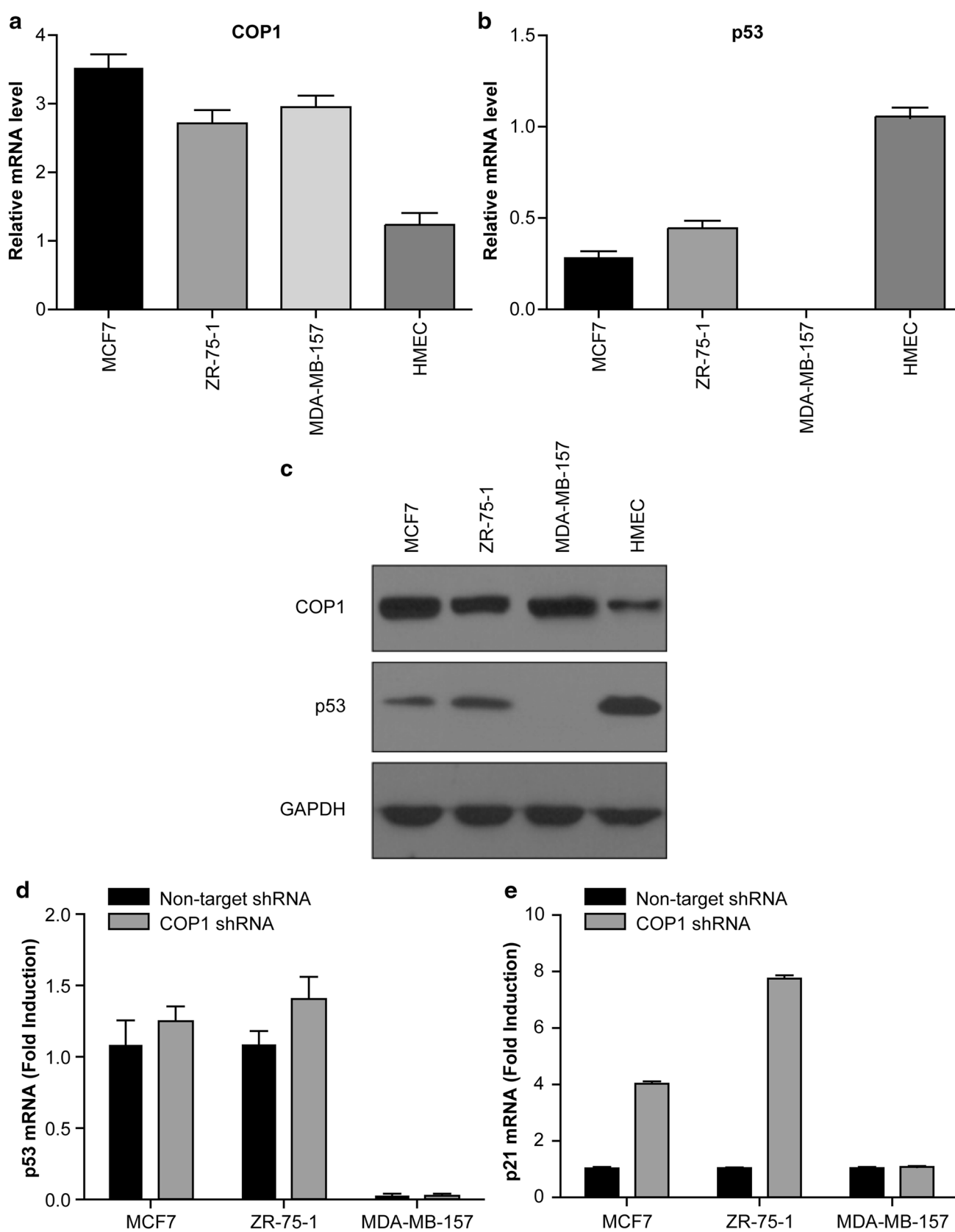


Fig. 1 Effect of *COP1* silencing on *p53* and *p21* expression. Endogenous *COP1* (a) and *p53* (b) mRNA levels in three BC cell lines (MCF7, ZR-75-1 and MDA-MB-157) were measured via quantitative PCR; expression levels in HMEC cells (non-cancerous) are equaled to 1 ($P < 0.05$). c Western blot analysis of COP1 and p53 levels in both BC cells and a non-cancerous cell line. Expression of *p53* (d) and *p21* (e) mRNA (normalized to *GAPDH*), upon COP1 knockdown ($P < 0.05$)

Analysis of cell cycle arrest

Cells were treated with 10 MOI *shCOP1* (or control shRNA) lentiviral particles for 72 h. To analyze cell cycle arrest, cells were fixed at 4 °C for 30 min in 70% ethanol and washed twice with phosphate-buffered saline (PBS) prior to treatment with 50 µL RNase A (100 µg/mL) and 200 µL PI (50 µg/mL stock solution). Flow cytometric analysis of the samples was conducted using a FACSCalibur instrument and the CellQuest software.

Caspase 3/7 assay

BC cell lines were seeded at a density of 1×10^4 cells/well in 96-well plates and allowed to attach overnight before being washed with PBS and infected (for 72 h) with 10 MOI *shCOP1* (or control shRNA) lentiviral particles. Caspase 3/7 activity was assayed by addition of the Caspase-Glo 3/7 chemiluminescence reagent (Promega) according to manufacturer instructions. Luminescence was measured using a Glomax multi-detection system (Promega).

MitoLight apoptosis-detection kit

Changes in mitochondrial-membrane potential were assayed using the MitoLight™ dye (Millipore). In healthy cells, the dye accumulates in the mitochondria, where it aggregates and produces a red fluorescent signal, while it remains in the monomeric form in the cytoplasm of apoptotic cells, producing a green-fluorescent signal. Cells (2.5×10^5 cells/well) were infected with *shCOP1* (or control shRNA) lentiviral particles (10 MOI) for 72 h and incubated for 30 min with 50 µL of pre-diluted MitoLight solution (900 µL water, 1 µL MitoLight dye, and 100 µL $10 \times$ incubation buffer) according to manufacturer instructions. A total of 10,000 cells per treatment were analyzed via flow cytometry and images of cells similarly treated were acquired using a Zeiss Axiovert 200 fluorescence microscope (Carl Zeiss, Oberkochen, Germany) with an AxioCam MRm camera and the Axiovision 3.1 software (Carl Zeiss), and cell images were analyzed using the Adobe Photoshop software (Adobe Systems, San Jose, CA, USA).

Quantification and statistical analysis

One-way analysis of variance was used to evaluate all data, and $P < 0.05$ was considered to indicate statistical significance. All statistical analyses were performed using the Prism 7.0 software (GraphPad Software, San Diego, CA, USA).

Results

Expression of COP1 and p53 in BC cell lines

We first identified the p53 genotype of the three BC cell lines used in this study. Sequencing of extracted full-length cDNAs revealed that two of the three cell lines (MCF7 and ZR-75-1) harbored WT *p53*, whereas MDA-MB-157 cells exhibited a *p53*-null phenotype based on undetectable *p53* expression.

We then investigated the expression of COP1 and p53 in three BC cell lines and one non-cancerous human mammary epithelial cell line (HMEC). By qPCR, we found that the expression of *COP1* was three to four times lower in the non-cancerous HMEC compared to the cancer cell lines (Fig. 1a), while *p53* was highly expressed in non-cancerous cells, compared with BC cells (Fig. 1b). Western blot assays gave similar results (Fig. 1c). These data showed that the degree of expression of COP1 and p53 was different depending on the cell line.

Next, we investigated the levels of p53 after *COP1* knockdown. Downregulation of *COP1* in the three BC cell lines was not associated to changes in the levels of *p53* mRNA (Fig. 1d). However, we found that *COP1* silencing affected the levels of the p53-effector p21, which changed in some of the cell lines investigated: upon *COP1* knockdown, the levels of *p21* increased 4 and 6.5 folds in MCF7 and ZR-75-1 BC cells (both harboring WT *p53*), respectively, as compared with control (cells in which *COP1* had not been knocked down). Contrarily, *COP1* knockdown in the BC cells harboring mutant *p53* did not alter *p21* mRNA levels (Fig. 1e). Furthermore, *COP1* silencing did not induce any changes in *p53* mRNA levels, consistent with previous studies reporting the *COP1*-mediated degradation of p53 protein, with no corresponding modulation of *p53* mRNA levels [23, 26]. These data indicate that COP1 is an E3 ubiquitin protein ligase that degrades the p53 protein and increases *p21* mRNA.

COP1 silencing inhibits BC cell viability

An MTT assay was used to investigate whether COP1 plays a role on cell viability. Infection of the cells with viral particles expressing *COP1* or control shRNA for 72 h indicated a dose-dependent reduction in the viability of the BC

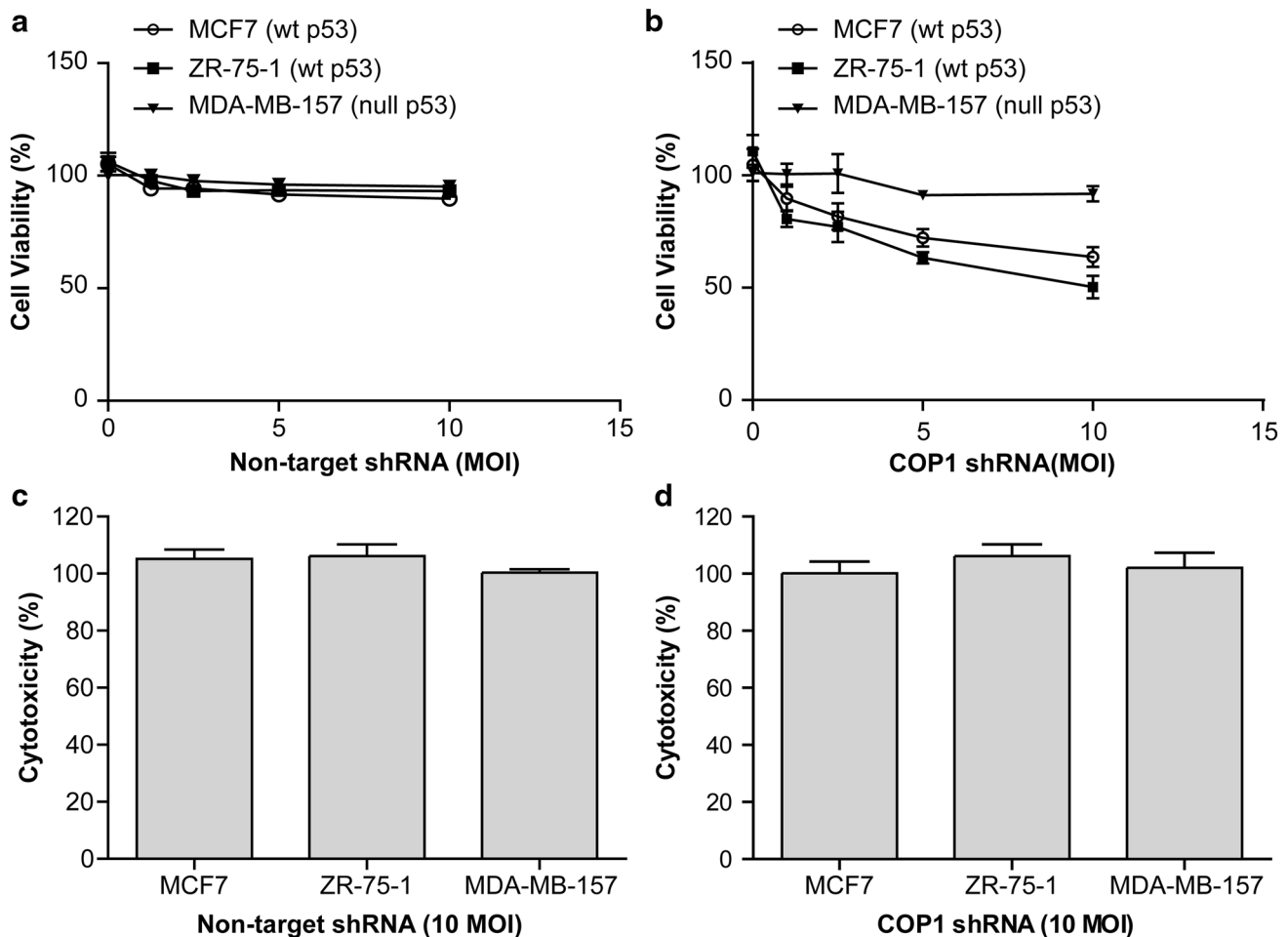


Fig. 2 Effect of *COP1* silencing on BC cell viability and toxicity. MCF7, ZR-75-1 and MDA-MB-157 cells were infected with 1, 2.5, 5, or 10 MOI lentiviral particles expressing non-silencing shRNA (**a**) or *shCOP1* (**b**) for 72 h. The percentage of viable cells, relative to

controls, was determined using an MTT assay ($P < 0.05$). Cytotoxicity in human BC cells infected with lentiviral particles expressing non-silencing shRNA (**c**) or *shCOP1* (**d**), as measured using an LDH assay

cells expressing WT *p53*: specifically, we found a 47 and 50% reduction of the viability in MCF7 and ZR-75-1 cells, respectively (Fig. 2a, b). By contrast, knockdown of *COP1* did not cause any significant change in the viability of MDA-MB-157 cells, suggesting that *COP1* silencing induced a *p53*-dependent decrease in cell viability. Furthermore, we assessed the cytotoxicity associated with the overexpression of *shCOP1* or of the non-targeting shRNA, and we did not find any (Fig. 2c, d). Therefore, the effects of *COP1* silencing on cell viability were dependent on *p53* status.

COP1 silencing activates the p53-mediated transcription

The tumor suppressor p53 has been shown to mediate various cellular processes, including gene transcription,

DNA repair, genome stability, senescence, cell cycle regulation, and apoptosis [15–23]. Therefore, we investigated the effect of *COP1* knockdown on the expression on p53-related proteins. We treated MCF7, ZR-75-1, and MDA-MB-157 cells with lentiviral particles (at 10 MOI) expressing *shCOP1* for 72 h to determine whether *COP1* silencing affects p53, and the expression of p-53 related proteins. Western blot analyses showed that p53, p21, and PUMA protein levels increased in response to *COP1* silencing in MCF7 and ZR-75-1 (Fig. 3a). Furthermore, we also observed a decrease in the expression of CDK2 concomitant to the increase in p21 levels, in agreement with previous studies demonstrating that p53-induced p21 inhibits the expression of CDK4 and CDK2 [10]. These findings demonstrate that *COP1* regulates p53 protein levels, thereby altering the expression of p53-target genes.

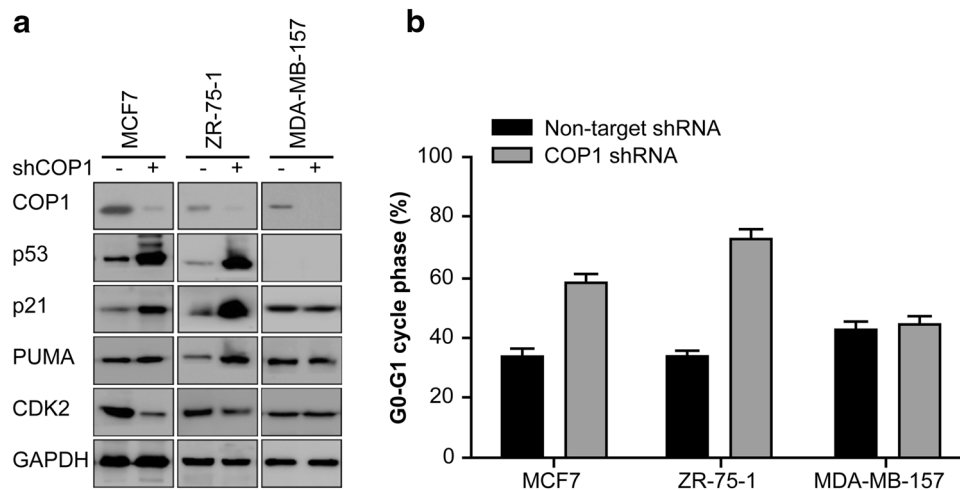


Fig. 3 *p53*-dependent cell cycle arrest upon *COP1* silencing. **a** Western blot analysis of the expression of the indicated proteins in BC cell lines expressing WT (MCF7 and ZR-75-1) or mutant (MDA-MB-157) *p53* following infection with lentiviral particles (10 MOI) expressing non-silencing shRNA or *shCOP1* for 72 h. GAPDH was

used as a loading control. **b** *COP1* positively regulates G_1 cell cycle arrest. G_0/G_1 -phase distribution was evaluated in BC cells infected with lentiviral particles (10 MOI) expressing non-silencing shRNA or *shCOP1* for 48 h ($P < 0.05$)

p53 activation promotes cell cycle arrest

To further investigate the role of *COP1*, we analyzed the effect of *COP1* silencing on cell cycle progression. We found that *COP1* silencing induced cell cycle arrest in human BC cells expressing WT *p53*. Specifically, knockdown of *COP1* was associated with the increase in the percentage of cells arrested in G_0/G_1 from 34 to 58% (1.7-fold) and from 31 to 70% (2.3-fold), in MCF7 and ZR-75-1 cells, respectively. By contrast, *COP1* silencing did not affect cell cycle progression in MDA-MB-157 cells (Fig. 3b). Therefore, inhibition of *COP1* expression in BC cells leads to an increase in *p53* and *p21* expression, thereby inhibiting the cell cycle.

COP1 induces apoptosis in a p53-dependent manner

Next, we investigated whether the overexpression of *p53*, caused by *COP1* silencing, induced cell death. First, we stained control or *COP1*-silenced cells with Annexin V and PI and analyzed the cells via flow cytometry. Viable cells are Annexin V- and PI-negative cells. Most of the control cells were viable. However, after *COP1* knockdown, the number of apoptotic cells (Annexin V-positive and PI-negative) increased in the BC cells with WT *p53*. Specifically, we observed a 2.4- and 4.0-fold increase in the number of apoptotic MCF7 and ZR-75-1 cells, respectively, as compared with the control cells (Fig. 4a). Contrarily, we did not observe any change in the number of apoptotic cells in the MDA-MB-157 cell line. Therefore, *COP1* silencing induces apoptosis in tumor-cell lines expressing WT *p53*.

Apoptosis is associated with mitochondrial fragmentation and depolarization. Therefore, we investigated whether knockdown of *COP1* was associated with changes in the mitochondrial-membrane potential, by staining the cells with the MitoLight™ dye. Following *COP1* silencing (72 h), MCF7 and ZR-75-1 cells exhibited increased cytoplasmic green-fluorescent signals (Fig. 4b), indicative of mitochondrial-membrane depolarization and apoptosis. Accordingly, these cells also exhibited a 6.7- and 10.8-fold increase in apoptosis, respectively (Fig. 4c); however, no significant increase in apoptosis was observed in the *p53*-null BC cell line. These results indicated that *COP1*-mediated *p53* degradation causes a *p53*-dependent depolarization of the mitochondrial-membrane potential, leading to apoptosis.

We then measured the activation of caspase-3 upon *COP1* silencing and found that knockdown of *COP1* was associated with elevated caspase-3/7 levels in the cells with WT *p53*. Specifically, caspase 3/7 levels were upregulated 0.6- and 1.3-fold in MCF7 and ZR-75-1 cells, respectively; however, they remained virtually unchanged in MDA-MB-157 cells (Fig. 4d), confirming that the apoptosis observed upon knockdown of *COP1* was dependent upon the presence of WT *p53*. These findings suggest that *COP1* mediates the ubiquitination and degradation of *p53* in the analyzed BC cell lines harboring WT *p53*. Therefore, knockdown of *COP1* causes the overexpression of *p53*, the upregulated transcription of *p53*-target genes, caspase-3/7 activation, and reduced tumor-cell viability.

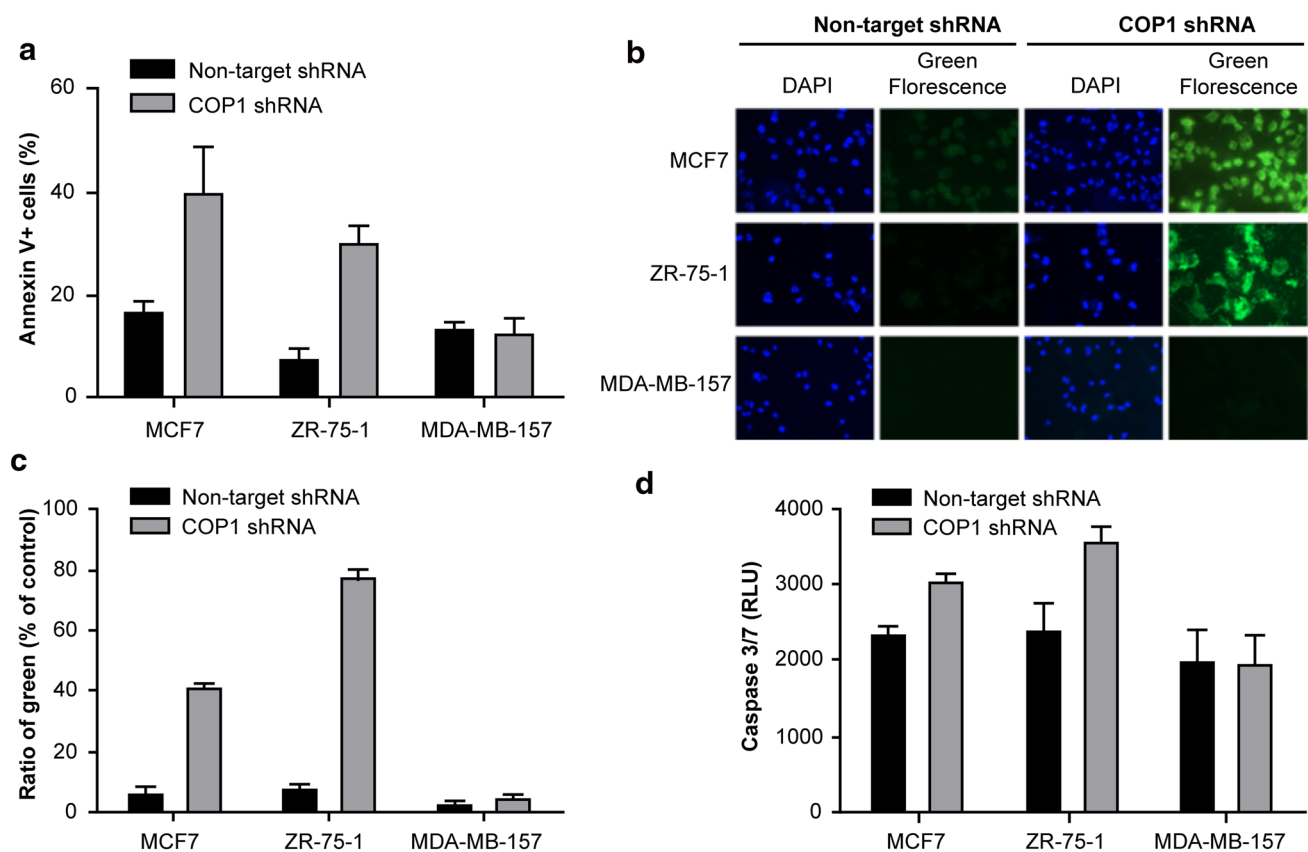


Fig. 4 *COP1* silencing induces apoptosis. **a** The viability of the three BC cell lines (MCF7, ZR-75-1 and MDA-MB-157) was analyzed by flow cytometry following infection with lentiviral particles (10 MOI) expressing non-silencing shRNA or *shCOP1* for 72 h. Cells were stained with Annexin V-FITC/PI. Effect of *COP1* silencing on the proportion of Annexin V-positive cells in the analyzed BC cell lines ($P < 0.05$ vs. untreated control). **b** Representative images of cells treated as described in **c**. **c** Changes in mitochondrial-membrane potential as assessed by staining with the MitoLight™ dye in BC cells infected with lentiviral particles (10 MOI) expressing non-silencing shRNA or *shCOP1* for 12 h. Apoptosis was determined

using fluorescence microscopy and flow cytometry. The observed red/green fluorescence ratio in cells was determined via flow cytometry. $P < 0.05$ as compared with green fluorescence levels observed in the control group. Experiments were performed in triplicate. **d** BC cell lines were infected with lentiviral particles (10 MOI) expressing non-silencing shRNA or *shCOP1* for 48 h and treated with the Caspase-Glo 3/7 reagent. Caspase-3/7 activation was assessed by monitoring the cleavage of the pro-luminescent caspase-3/7 substrate. Data represent the mean \pm standard deviation for experiments performed in triplicate ($P < 0.05$). RLU relative luminescence unit

Discussion

COP1, overexpressed in several cancer cell lines, promotes the proteasomal degradation of the tumor suppressor p53 [17]. In some cancer types, COP1 levels are strongly correlated with increased cancer progression and tumorigenesis [16, 19–22, 27–29]; however, the functional role of COP1 in human tumors is cell-type dependent and remains controversial [4, 7]. Furthermore, the functional and/or mechanistic role of COP1 in human BC is unclear. In this study, we used RNA interference to investigate the COP1-mediated regulation of p53 in cultured human BC cells.

Our results showed that COP1 “suppression/silencing” stabilized and activated p53 in BC cell lines harboring WT p53, leading to p53-dependent cell cycle arrest and apoptosis. Specifically, p53 activation was associated to the

increased expression of *p21* and other pro-apoptotic genes, as well as the inhibition of *CDK2* expression (Fig. 3a). By contrast, knockdown of *COP1* expression had no effect on either cell cycle arrest or apoptosis in the BC cell line harboring the mutant *p53* variant, indicating that the observed effect of COP1 was dependent on *p53* status.

Previous studies demonstrate that *COP1* acts as an oncogene and can suppress p53 activity [21, 22, 28]. The interaction between COP1 and p53 and the role of COP1 as a negative regulator of p53 have been confirmed in immunoprecipitation assays [19, 25]. COP1 overexpression in BC cells attenuates p53 protein levels, thereby facilitating tumor progression. As an E3 ubiquitin ligase, indeed, COP1 suppresses p53 by inducing its proteasomal degradation [19, 23, 25]. Additionally, in BC cells, COP1 acts with glycogen synthase kinase 3 β to promote c-Jun

degradation, thereby inhibiting tumorigenesis [28]. Nevertheless, the consequences of the COP1/p53 interaction in BC are not fully understood, yet. Therefore, this study investigated the relationship between COP1 and p53. Our data point to COP1 as a potential BC therapeutic target. We show that *COP1* silencing induces an increase in both p53 protein production and p53-target gene transcription in MCF7 and ZR-75-1 cells, both of which harbor WT *p53* (Fig. 3a). These changes were not observed in the *p53*-null MDA-MB-157 cells in response to *COP1* silencing, suggesting that COP1 might mediate cancer progression by attenuating p53 levels. Additionally, we found that knockdown of *COP1* did not affect the levels of *p53* mRNA, while it increased those of *p21* (Fig. 1d, e). These results are consistent with those of previous studies, which show that the COP1-mediated inhibition of p53 occurs via the induction of the ubiquitination-mediated proteasomal degradation of p53, rather than through direct effects on *p53* mRNA levels [13, 15, 27, 28].

COP1-mediated apoptosis was confirmed via MTT assays. Furthermore, apoptosis and cell cycle arrest occurred upon *COP1* silencing in the cell lines harboring WT *p53* (MCF7 and ZR-75-1); no change in the apoptosis rate was detected in *p53*-null MDA-MB-157 cells. p53 regulates *p21* mRNA levels through its nuclear accumulation [24, 25]. Given that *p53* promotes G₁ arrest via the induction of *p21* expression, and that p53 and p21 levels were increased in response to knockdown of *COP1* in BC cells with WT *p53*, we concluded that *COP1* silencing induces cell cycle arrest and apoptosis via the accumulation of p53 and the activation of the p53 pathway. The difference in the G₀/G₁ arrest observed in MCF7 and ZR-75-1 cells was most likely due to differences in gene expression. Specifically, MCF7 cells have higher levels of the p53 repressor MDM2/murine double minute X (MDMX) than ZR-75-1 cells and differences in the serine phosphorylation levels of p53, which might affect its interaction with the DNA [30, 31].

In summary, our results demonstrate that *COP1* silencing promotes p53 accumulation, leading to cell cycle arrest, mitochondrial-membrane depolarization, caspase activation, and p53-dependent cell death. These data strongly suggest that silencing of *COP1* is an effective strategy to inhibit BC cell proliferation by inducing apoptosis in cells expressing *p53*. Our findings indicate that inhibition of COP1 is a new way to modulate p53 activity and identify COP1 as a novel candidate therapeutic agent for the treatment of BC.

Compliance with ethical standards

Conflict of interest The authors declare no conflict of interest.

References

- Shah R, Rosso K, Nathanson SD. Pathogenesis, prevention, diagnosis and treatment of breast cancer. *World J Clin Oncol*. 2014;5(3):283–98. <https://doi.org/10.5306/wjco.v5.i3.283>.
- Harbeck N, Gnant M. Interpretation of the evidence for the efficacy and safety of statin therapy. *Lancet*. 2017;389(10074):1134–50. [https://doi.org/10.1016/S0140-6736\(16\)31891-8](https://doi.org/10.1016/S0140-6736(16)31891-8).
- Toledo F, Wahl GM. Regulating the p53 pathway: in vitro hypotheses, in vivo veritas. *Nat Rev Cancer*. 2006;6:909–23. <https://doi.org/10.1038/nrc2012>.
- Vousden KH, Prives C. Blinded by the light: the growing complexity of p53. *Cell*. 2009;137:413–31. <https://doi.org/10.1016/j.cell.2009.04.037>.
- Gu L, Zhu N, Findley HW, Zhou M. MDM2 antagonist nutlin-3 is a potent inducer of apoptosis in pediatric acute lymphoblastic leukemia cells with wild-type p53 and overexpression of MDM2. *Leukemia*. 2008;22:730–9. <https://doi.org/10.1038/leu.2008.11>.
- Bargonetti J, Manfredi JJ. Multiple roles of the tumor suppressor p53. *Curr Opin Oncol*. 2002;14:86–91. <https://doi.org/10.1097/00001622-200201000-00015>.
- Teodoro JG, Evans SK, Green MR. Inhibition of tumor angiogenesis by p53: a new role for the guardian of the genome. *J Mol Med (Berl)*. 2007;85:1175–86. <https://doi.org/10.1007/s00109-007-0221-2>.
- Fridman JS, Lowe SW. Control of apoptosis by p53. *Oncogene*. 2003;22:9030–40. <https://doi.org/10.1038/sj.onc.1207116>.
- Vogelstein B, Lane D, Levine AJ. Surfing the p53 network. *Nature*. 2000;408:307–10. <https://doi.org/10.1038/35042675>.
- He G, Siddik ZH, Huang Z, Wang R, Koomen J, Kobayashi R, et al. Induction of p21 by p53 following DNA damage inhibits both Cdk4 and Cdk2 activities. *Oncogene*. 2005;24:2929–43. <https://doi.org/10.1038/sj.onc.1208474>.
- Nilausen K, Green H. Reversible arrest of growth in G₁ of an established fibroblast line (3T3). *Exp Cell Res*. 1965;40:166–8. [https://doi.org/10.1016/0014-4827\(65\)90306-X](https://doi.org/10.1016/0014-4827(65)90306-X).
- Bianchi E, Denti S, Catena R, Rossetti G, Polo S, Gasparian S, et al. Characterization of human constitutive photomorphogenesis protein 1, a RING finger ubiquitin ligase that interacts with Jun transcription factors and modulates their transcriptional activity. *J Biol Chem*. 2003;278:19682–90. <https://doi.org/10.1074/jbc.M212681200>.
- Jain AK, Barton MC. Making sense of ubiquitin ligases that regulate p53. *Cancer Biol Ther*. 2010;10:665–72. <https://doi.org/10.4161/cbt.10.7.13445>.
- Deng XW, Caspar T, Quail PH. COP1: a regulatory locus involved in light-controlled development and gene expression in Arabidopsis. *Genes Dev*. 1991;5:1172–82. <https://doi.org/10.1101/gad.5.7.1172>.
- Choi HH, Phan L, Chou PC, Su CH, Yeung SC, Chen JS, et al. COP1 enhances ubiquitin-mediated degradation of p27Kip1 to promote cancer cell growth. *Oncotarget*. 2015;6:19721–34. <https://doi.org/10.18632/oncotarget.3821>.
- Vitari AC, Leong KG, Newton K, Yee C, O'Rourke K, Liu J, et al. COP1 is a tumor suppressor that causes degradation of ETS transcription factors. *Nature*. 2011;474:403–6. <https://doi.org/10.1038/nature10005>.
- Li YF, Wang DD, Zhao BW, Wang W, Huang CY, Chen YM, et al. High level of COP1 expression is associated with poor prognosis in primary gastric cancer. *Int J Biol Sci*. 2012;8:1168–77. <https://doi.org/10.7150/ijbs.4778>.
- Marine JC. Spotlight on the role of COP1 in tumorigenesis. *Nat Rev Cancer*. 2012;12:455–64. <https://doi.org/10.1038/nrc3271>.
- Dornan D, Bheddah S, Newton K, Ince W, Frantz GD, Dowd P, et al. COP1, the negative regulator of p53, is overexpressed in

- breast and ovarian adenocarcinomas. *Cancer Res.* 2004;64:7226–30. <https://doi.org/10.1158/0008-5472.CAN-04-2601>.
20. Ouyang M, Wang H, Ma J, Lu W, Li J, Yao C, et al. COP1, the negative regulator of ETV1, influences prognosis in triple-negative breast cancer. *BMC Cancer.* 2015;15:132. <https://doi.org/10.1186/s12885-015-1151-y>.
 21. Lu G, Zhang Q, Huang Y, Song J, Tomaino R, Ehrenberger T, et al. Phosphorylation of ETS1 by Src family kinases prevents its recognition by the COP1 tumor suppressor. *Cancer Cell.* 2014;26:222–34. <https://doi.org/10.1016/j.ccr.2014.06.026>.
 22. Kato S, Ding J, Pisek E, Jhala US, Du K. COP1 functions as a FoxO1 ubiquitin E3 ligase to regulate FoxO1-mediated gene expression. *J Biol Chem.* 2008;283:35464–73. <https://doi.org/10.1074/jbc.M801011200>.
 23. Wang L, He G, Zhang P, Wang X, Jiang M, Yu L. Interplay between MDM2, MDMX, PIRH2, and COP1: the negative regulators of p53. *Mol Biol Rep.* 2011;38:229–36. <https://doi.org/10.1007/s11033-010-0099-x>.
 24. Tovar C, Rosinski J, Filipovic Z, Higgins B, Kolinsky K, Hilton H, et al. Small-molecule MDM2 antagonists reveal aberrant p53 signaling in cancer: implications for therapy. *Proc Natl Acad Sci USA.* 2006;103:1888–93. <https://doi.org/10.1073/pnas.0507493103>.
 25. Dornan D, Wertz I, Shimizu H, Arnott D, Frantz GD, Dowd P, et al. The ubiquitin ligase COP1 is a critical negative regulator of p53. *Nature.* 2004;429:86–92.
 26. Corcoran CA, Huang Y, Sheikh MS. The p53 paddy wagon: COP1, PIRH2, and MDM2 are found resisting apoptosis and growth arrest. *Cancer Biol Ther.* 2004;3:721–5. <https://doi.org/10.1038/nature02514>.
 27. Wertz IE, O'Rourke KM, Zhang Z, Dornan D, Arnott D, Deshaies RJ, et al. Human de-etiolated-1 regulates c-Jun by assembling a CUL4A ubiquitin ligase. *Science.* 2004;303:1371–4. <https://doi.org/10.1126/science.1093549>.
 28. Shao J, Teng Y, Padia R, Hong S, Noh H, Xie X, et al. COP1 and GSK3 β cooperate to promote c-Jun degradation and inhibit breast cancer cell tumorigenesis. *Neoplasia.* 2013;15:1075–85. <https://doi.org/10.1593/neo.13966>.
 29. Li DQ, Ohshiro K, Reddy SD, Pakala SB, Lee MH, Zhang Y, et al. E3 ubiquitin ligase COP1 regulates the stability and functions of MTA1. *Proc Natl Acad Sci USA.* 2009;106:17493–8. <https://doi.org/10.1073/pnas.0908027106>.
 30. Ray D, Murphy KR, Gal S. The DNA binding and accumulation of p53 from breast cancer cell lines and the link with serine 15 phosphorylation. *Cancer Biol Ther.* 2012;13:848–57. <https://doi.org/10.4161/cbt.20835>.
 31. Graves B, Thompson T, Xia M, Janson C, Lukacs C, Deo D, et al. Activation of the p53 pathway by small-molecule-induced MDM2 and MDMX dimerization. *Proc Natl Acad Sci USA.* 2012;109:11788–93. <https://doi.org/10.1073/pnas.1203789109>.